

ROBUST LASER-ULTRASONIC INTERFEROMETER BASED ON RANDOM QUADRATURE DEMODULATION

B.Pouet, S.Breugnot and P. Clémenceau

Bossa Nova Technologies; Venice, CA, USA

ABSTRACT. The new interferometric scheme that was presented at last year QNDE conference for robust and sensitive detection of ultrasound in industrial environment has been further improved. The proposed architecture combines quadrature detection with detector arrays for multi-speckle processing. The quadrature is reached thanks to the random phase distribution of the speckle light and the parallel signal processing is simplified by using an approximated demodulation technique based on signal rectification. Results demonstrating this new principle of operation and its performances are presented.

Keywords: Speckle, ultrasound, quadrature, interferometer, laser.

PACS: 43.35.Yb; 42.25.Hz; 42.30.Ms; 81.70Cv; 43.58.+z

INTRODUCTION

Various types of interferometer have been developed over the last 30 years for the measurement of small transient surface displacements, like the ones generated by ultrasonic waves. Various optical techniques have been extensively reviewed [1-3]. Most recently, a number of adaptive or compensated laser-based ultrasonic (LBU) receivers using photorefractive crystals have been developed. In the two most common approaches, the crystal is either used as a real-time hologram via two-wave mixing [4] or as a compensated photodetector via the photo-induced electromotive force (photo-EMF) effect [5]. Adaptive interferometers are mainly used in R&D laboratories. They have not yet been integrated into industrial inspection system, mainly because of their limited response time or, in the case of very fast adaptive systems based on photo-EMF, of their very limited sensitivity.

To date, the few successful integration of LBU industrial inspection systems are still mostly based on the confocal Fabry-Pérot interferometer [6,7]. In order to become more broadly used as an on-line measurement tool, LBU still needs more rugged, compact and cost effective solutions [8,9].

We present here the latest results in the development of a new type of interferometric receiver specifically designed to respond to needs associated with LBU measurement in industrial environments. Preliminary results were presented at last year QNDE conference [9]. The system previously presented uses a quadrature interferometric detection scheme that delivers two, in quadrature, electronic signals and the surface motion was extracted using either a linear-displacement demodulator or a displacement-square

demodulator. The ability to detect on optically rough surfaces was achieved with the use of detector arrays and parallel processing of the multi-signals. This multi-channel quadrature interferometer has been further improved and we now present a novel configuration using a simplified optical setup and a simpler signal demodulation that is optimized for high density parallel processing. These interferometer simplifications directly translate into a more compact, robust and cost effective system, without reducing its sensitivity to ultrasound.

QUADRATURE INTERFEROMETER

Quadrature interferometers rely on the detection of two interference fields that are 90° out of phase. Various optical set-up can be used in order to achieve this 90° phase difference. Figure 1 shows an example of an optical setup where the 90° phase difference is introduced by interfering a circularly polarized reference beam and a linearly polarized object beam. The intensity on detectors (1) and (2) can be expressed as:

$$I_1 = I_{av} (1 + \alpha \text{Sin}[\phi_{LF}(t, x) + \phi_{UT}(t)]) \quad \text{and} \quad I_2 = I_{av} (1 + \alpha \text{Cos}[\phi_{LF}(t, x) + \phi_{UT}(t)]) \quad (1)$$

Where $\phi_{LF}(t, x)$ is the low frequency component of phase, fluctuating between 0 and 2π . It includes the spatial variation from the speckle and the time variation caused by disturbance such as: air current, vibration, whole body motion or thermal gradient. $\phi_{UT}(t) = 4\pi\delta(t)/\lambda$ is the high-frequency and small-amplitude variation of the phase caused by the ultrasonic displacement $\delta(t)$. This phase variation is spatially coherent. I_{av} is the average intensity on the detector and α the modulation depth.

For accurate quadrature detection, the two detectors must see exactly the same interference field with only a 90° difference. For inspection on rough surfaces, this means that the two detectors must see the same speckle. This can be achieved by careful alignment of the detectors. In order to increase the interferometer sensitivity and to reduce the signal drop-outs we previously showed that single detectors can be advantageously replaced by detector arrays [9]. The alignment procedure used with single detectors also applies to detector arrays. The use of detector arrays instead of single detectors does not complicate the optical setup or the alignment procedure. Detector arrays are used with parallel processing for demodulation of every channel before summation of all the demodulated signals in order to generate the stable output signal.

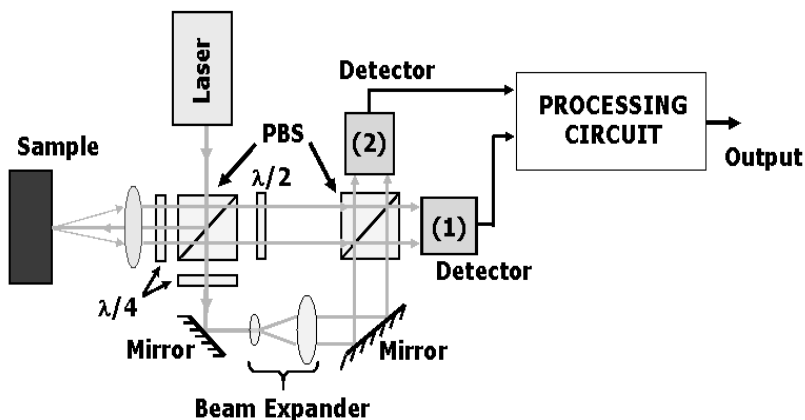


FIGURE 1. Schematic of quadrature detection interferometer.

The use of a demodulation scheme requiring fewer components is preferred because it will lead to simpler integration for the high density parallel processing.

DEMODULATION

Various demodulations have been proposed in order to extract the ultrasonic information $\phi_{UT}(t)$ [1]. Depending on the selected demodulation, the output signal can be chosen to be proportional to the surface displacement, velocity or displacement-square. The velocity demodulation and the displacement demodulation will not be studied here as they require a more complex electronic circuitry and are thus not well suited for use with detector arrays and parallel processing [9].

Square Demodulation

The schematic for displacement-square demodulation is shown in Figure 2A. First the detector signals are high-pass filtered to remove low frequency variation $\phi_{LF}(t)$. After high-pass filtering, the signals V_1 and V_2 can be expressed as:

$$V_1 = \alpha I_{av} \text{Cos}[\phi_{LF}(t, x)] \times \phi_{UT}(t) \quad \text{and} \quad V_2 = -\alpha I_{av} \text{Sin}[\phi_{LF}(t, x)] \times \phi_{UT}(t). \quad (2)$$

Where we have assumed that the ultrasonic displacement $\delta(t)$ is small compared to the optical wavelength λ . Both signal are then squared and summed leading to the output signal V_{out} :

$$V_{out} = [\alpha I_{av}]^2 [\phi_{UT}(t)]^2. \quad (3)$$

From Eq.3 we see that the low frequency phase fluctuation has been rejected and does not influence the output signal. The squaring function is implemented using multiplier circuits. For many years, the multiplier circuits have been the limiting factor for the development of sensitive quadrature interferometer but high-speed and low noise multipliers are now commercially available. For example, the AD834 from Analog Devices has a bandwidth up to 500MHz and an output noise spectral density as low as $16nV/\sqrt{Hz}$.

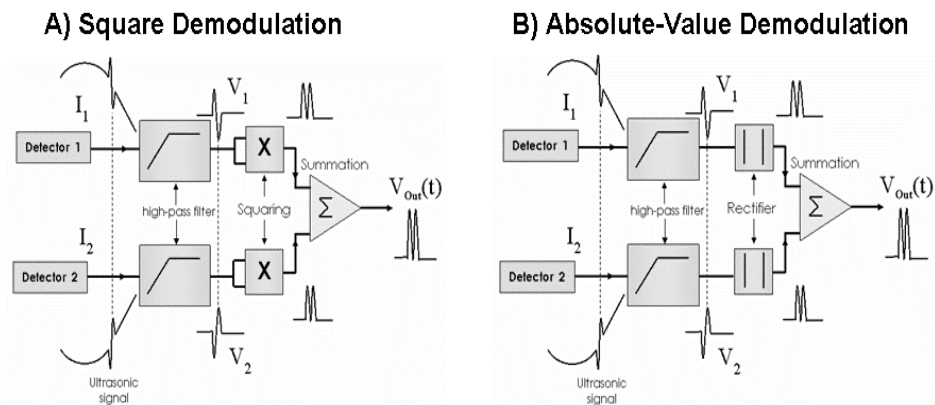


FIGURE 2. Demodulation of quadrature signals: A) Square-displacement demodulation and B) Absolute-value (rectification) displacement demodulation.

Approximated Demodulation

For high density parallel processing that is needed when using detector array with large number of element, an approximated-demodulation is preferred to the square demodulation. Indeed, multiplier circuits are pricy components and their packaging choice is limited, making very compact design a challenge. Furthermore, the squaring process reduces the signal dynamic and it makes the detection of small amplitude signal in the presence of large amplitude signal more difficult. Instead, an approximated demodulation based on signal rectification can be implemented. Rectification is much simpler to implement electronically that squaring and it does not suffer the reduction in signal dynamic. Furthermore, a rectifier can be built with a variety of off-the-shelf low cost electronic components, facilitating the integration into high density compact processing circuits.

As shown Figure 2B, the approximated demodulation uses a similar configuration than the square demodulation. The squaring is now replaced by a rectifier. The high-pass filtered signals (eq.2) are rectified, summed and the output signal V_{out} becomes:

$$V_{out} = \alpha I_{av} [|\text{Sin}(\phi_{LF}(t,x))| + |\text{Cos}(\phi_{LF}(t,x))|] \cdot |\phi_{UT}(t)|. \quad (4)$$

The output signal now has a small dependency on $\phi_{LF}(t,x)$. This dependency is not critical because it always leads to a strong signal and the amplitude variation stays moderate: $1 \leq |\text{Sin}\phi| + |\text{Cos}\phi| \leq \sqrt{2}$.

RANDOM QUADRATURE

For industrial application, an optical system requiring no accurate alignment will be preferred because of its intrinsic robustness, reduced maintenance and lower manufacturing cost. The system described earlier, where two interference fields with a 90° phase shift must be detected, may not be the best suited for integration in an industrial system. A configuration where no critical alignment is required will be preferred. This can be achieved by taking advantage of the random nature of speckles. As shown on Figure 3, the interferometric scheme is now simplified by removing the quadrature detection. Only one detector array is now needed. It must be noted that a second detector array can be used to detect the second interference field available after the beam splitter, but it is not mandatory for operation of the interferometer.

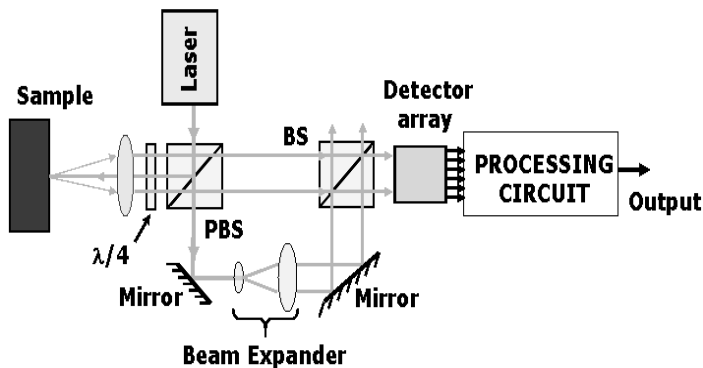


FIGURE 3. Schematic of the simplified interferometer for random quadrature detection.

The signal from an element of the photodiode array is:

$$I_x = I_{ref}(1 + \alpha_x \text{Sin}[\phi_{LF}(t, x) + \phi_{UT}(t)]). \quad (5)$$

Here, we have assumed that the intensity of the reference beam, I_{ref} is much stronger than the intensity of the scattered object beam I_x and thus, the average intensity I_{av} on the photodiode elements is not dependent on the object beam intensity. The modulation factor α_x can be expressed as: $\alpha_x = 2\sqrt{I_x/I_{ref}}$. After high-pass filtering and rectification the elementary signal becomes:

$$V_x = \alpha_x I_{ref} |\text{Cos}[\phi_{LF}(t, x)]| \times |\phi_{UT}(t)|. \quad (6)$$

The elementary signals are then summed to generate the output signal V_{out} :

$$V_{out} = I_{ref} \times |\phi_{UT}(t)| \times \sum_N \alpha_x |\text{Cos}(\phi_{LF}(t, x))|. \quad (7)$$

N corresponds of the number of elements in the photodiode array. We have assumed here that the speckle is fully resolved by the detector array (the size of the detector element \leq speckle size). From the speckle statistics we know that the speckle intensity follows a negative exponential function and that the phase is equally distributed [10]. It follows that for a very large number of detector elements N , the output signal V_{out} averages out to:

$$V_{out} = \left(\frac{4N}{\pi}\right) \sqrt{I_{(Speckle)} I_{ref}} \times |\phi_{UT}(t)|. \quad (8)$$

Where $I_{(Speckle)}$ is the average intensity of a speckle. For comparison, the very best sensitivity that could be reached by using an “ideal” stabilized Michelson interferometer, capable to stabilize for every speckle, will lead to the maximum output signal:

$$V_{Ideal} = 2N \sqrt{I_{(Speckle)} I_{ref}} \times \phi_{UT}(t). \quad (9)$$

The sensitivity of this multi-channel random-quadrature interferometer exhibits a near ideal sensitivity, showing only a sensitivity reduction by $(2/\pi)$ compared to the ideal case.

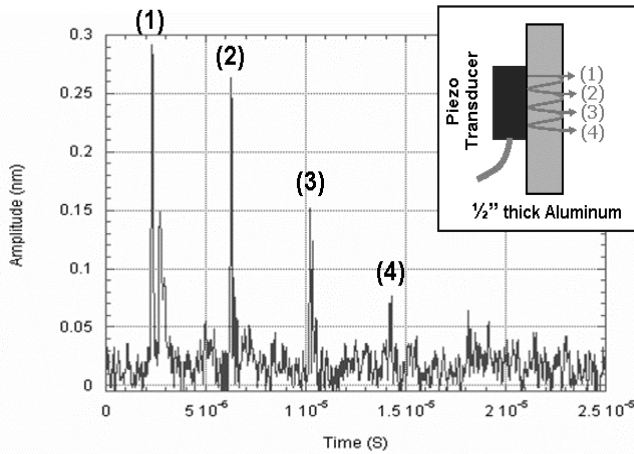


FIGURE 4. Ultrasonic surface displacement measured by the 25-channel random-quadrature interferometer. The ultrasonic pulse is generated by a 5MHz transducer propagating through a 1/2” inch thick aluminium plate. Single shot measurement with the maximum displacement corresponding to 0.3nm. The aluminium surface was sandblasted in order to get a uniform optically rough surface.

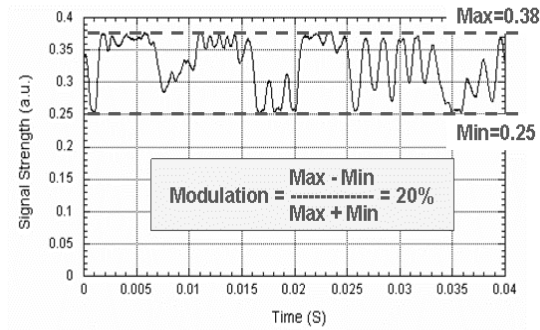


FIGURE 5. Low frequency variation of the signal amplitude due to the small number (25) of independent signals used to average out the random speckle phase.

An example of ultrasonic signals recorded with the 25-channel random-quadrature interferometer is shown in Figure 4. A small amplitude ultrasonic pulse is generated by a standard 5MHz, 1/2" diameter, piezoelectric transducer attached to a 1/2" inch thick aluminium plate. The sample surface was sandblasted in order to get a uniform optically rough surface. The 25-channel random-quadrature interferometer uses a 70mW laser at $\lambda=532\text{nm}$. Figure 4 shows a single shot signal acquired with a detection bandwidth [100kHz – 10MHz]. The maximum displacement amplitude of the first echo corresponds to 0.3nm. Four echoes are clearly visible.

As indicated earlier, this interferometric scheme uses averaging from multi-detection of randomly distributed speckles in order to get a stable demodulated signal. Figure 5 shows the fluctuation of the output signal from the 25-channel interferometer when the speckle phase was made to fluctuate more than 2π by introducing external perturbations. As shown in Figure 5, despite the small number of detectors (25) used for averaging out the random speckle phase distribution, the signal amplitude is fairly stable and fluctuates by no more than about 20%. It must be noted that the 20% variation of the signal amplitude due to the random demodulation process is still much less than the signal variation caused by the intensity variation in the back scattered light generally encountered when scanning across an optically rough surface. For example, on a rough aluminum sample we found about 60% intensity variation in the backscattered light when scanning the probe beam across the surface.

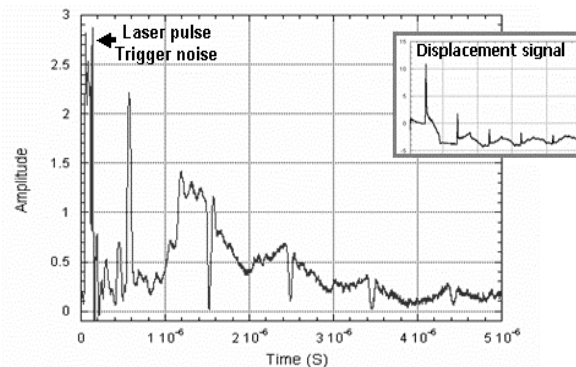


FIGURE 6. Laser ultrasonic rectified displacement measured by the 25-channel random-quadrature interferometer (the signal recorded by a displacement interferometer is also shown for comparison). The ultrasonic pulse is generated by a pulsed Nd:Yag laser. 3mm thick aluminium sample.

Finally, an example of laser ultrasonic signals recorded with the 25-channel random-quadrature interferometer is shown in Figure 6. In this experiment, ultrasounds were generated in a 3mm thick aluminum plate by laser ablation resulting from the absorption of a 100mJ, 10nS pulse of a Nd:YAG laser @1.06 μ m. Figure 6 shows the detected signal corresponding to the through-transmission geometry. The detection bandwidth was [100kHz-10MHz] and the 1st echo amplitude corresponds to 2nm displacement. For comparison, the surface displacement was also measured with an adaptive photorefractive two-wave mixing interferometer that delivers an output signal proportional to the surface displacement. As expected, the signal from the 25-channel random-quadrature interferometer corresponds to the absolute value of the surface displacement.

CONCLUSION

By taking advantage of the speckle statistics, a robust, compact and cost-effective multi-channel interferometers can be implemented. The optical system is highly simplified using only one detector array. The electronic circuitry performing the parallel signal processing is also simplified by using an approximated demodulation scheme that is based on signal rectification. The stability of the output signal is now achieved by using a large number of channels and summing the demodulated signals. We demonstrated that an interferometer prototype using a 25-element detector array already exhibits a quite stable signal, with only about 20% of amplitude variation due to the speckle phase fluctuation. The stability and sensitivity achieved with this 25-channel interferometer makes it very well suited for a cost effective solution.

ACKNOWLEDGEMENTS

This work was supported by the National Science Foundation, DMI-0319425

REFERENCES

1. Scruby C.B. and Drain L.E., "*Laser Ultrasonics: Techniques and applications*", eds Adam Hilger, Bristol, UK 1990.
2. Monchalin J.-P., *Review of Progress in QNDE*, Vol 12, eds. D. O. Thompson and D. E. Chimenti, Plenum, New York, 1993, p. 495.
3. Dewhurst R. J. and Shan Q., *Meas. Sci. Technol.* Vol.10, 1999, p. 139.
4. Ing R.K. and Monchalin J.-P., *Appl. Phys. Lett.* Vol. 59, 1991, p. 3233.
5. Pouet B. F. et al., "On-machine characterization of moving paper using a photo-emf laser ultrasonics method", in *Process Control and Sensors for Manufacturing II*, SPIE Vol. 3589, 1999, p. 160.
6. Fiedler C. J., in *Review of Progress in QNDE*, Vol 20, eds. D. O. Thompson and D. E. Chimenti, Plenum, New York, 2001, p. 308.
7. Monchalin J.-P. et al, in *Review of Progress in QNDE*, Vol 22, eds. D. O. Thompson and D. E. Chimenti, Plenum, New York, 2003, p. 264.
8. Blouin A. et al, "Simple Laser-ultrasonic system using a single-frequency pulsed laser oscillator", in *Review of Progress in QNDE 24A*, edited by D. O. Thompson and D. E. Chimenti, AIP Conference Proceedings Vol.760, Melville, NY, 2005, pp. 265-272.
9. Pouet B. et al., "An innovative interferometer for industrial laser ultrasonic inspection" in *Review of Progress in QNDE 24A*, edited by D. O. Thompson and D. E. Chimenti, AIP Conference Proceedings Vol.760, Melville, NY, 2005, pp. 273-280.
10. J.W. Goodman, in *Laser speckle and related Phenomena*, 2nd ed., J.C. Dainty, ed., Vol. 9 of Springer Series in Topics in Applied Physics, Springer-Verlag, Berlin, 1984, p.9.